Communication

Molecular Engineering of Coaxial Donor–Acceptor Heterojunction by Coassembly of Two Different Hexabenzocoronenes: Graphitic Nanotubes with Enhanced Photoconducting Properties

Yohei Yamamoto, Takanori Fukushima, Akinori Saeki,
Shu Seki, Seiichi Tagawa, Noriyuki Ishii, and Takuzo Aida

J. Am. Chem. Soc., **2007**, 129 (30), 9276-9277• DOI: 10.1021/ja073577q • Publication Date (Web): 10 July 2007

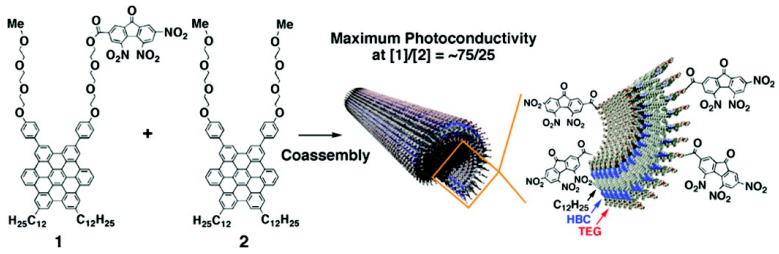

More About This Article

Additional resources and features associated with this article are available within the HTML version:

- Supporting Information
- Links to the 15 articles that cite this article, as of the time of this article download
- Access to high resolution figures
- Links to articles and content related to this article
- Copyright permission to reproduce figures and/or text from this article

View the Full Text HTML

J|A|C|S
COMMUNICATIONS

Published on Web 07/10/2007

Molecular Engineering of Coaxial Donor−Acceptor Heterojunction by Coassembly of Two Different Hexabenzocoronenes: Graphitic Nanotubes with Enhanced Photoconducting Properties

Yohei Yamamoto,[†] Takanori Fukushima,*[,†,‡] Akinori Saeki,[§] Shu Seki,[§] Seiichi Tagawa,[§] Noriyuki Ishii,[#] and Takuzo Aida*[,†,‡]

ERATO−SORST Nanospace Project, Japan Science and Technology Agency (JST), National Museum of Emerging Science and Innovation, 2-41 Aomi, Koto-ku, Tokyo 135-0064, Department of Chemistry and Biotechnology, School of Engineering, and Center for NanoBio Integration, The University of Tokyo, 7-3-1 Hongo, Bunkyo-ku, Tokyo 113-8656, Japan, Institute of Scientific and Industrial Research, Osaka University, 8-1 Mihogaoka, Ibaraki, Osaka 567-0047, Japan, and Biological Information Research Center, National Institute of Advanced Industrial Science and Technology (AIST), Tsukuba Central-6, 1-1-1 Higashi, Tsukuba, Ibaraki 305-8566, Japan

Received May 18, 2007; E-mail: fukushima@nanospace.miraikan.jst.go.jp; aida@macro.t.u-tokyo.ac.jp

Heterojunction of electron donor and acceptor molecular arrays within an electron-transferable distance is considered essential for organic photovoltaics and related fields.[1] This configuration is expected to allow for effective transport of photochemically generated carriers in the individual arrays by suppression of charge recombination. However, few examples of molecularly engineered nanoscale heterojunctions have so far been developed.[2] Recently, we found that a trinitrofluorenone (TNF)-appended hexa-*peri*-hexabenzocoronene (HBC) derivative (**1**) self-assembles to form a nanotubular object, where an electron-donating graphitic layer of π-stacked HBC is laminated by an electron-accepting molecular layer of TNF.[3] The coaxial graphitic nanotube is photoconductive with an excellent on/off ratio of 10^4. Nevertheless, it was uncertain if the current nanotubular structure is indeed optimum for the efficient photoconduction, since a higher level of acceptor doping, which is generally favorable for the forward electron transfer, can enhance the probability of charge recombination. Being motivated by this consideration, we explored coassembly[4a] of **1** and a HBC derivative without TNF (**2**)[4b] for fabricating coaxial graphitic nanotubes with varying TNF concentrations. This was really challenging, because the size regimes of their homotropic nanotubes are different from one another.[3,4b] Here we report that they can tubularly coassemble over a wide molar ratio (Figure 1). We also highlight that the coassembly enables a much better photoconductivity than that of the homotropic nanotubes of **1**.

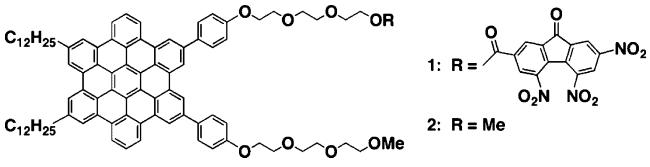

A 9 mL vial containing a THF solution (4 mL) of a 1:1 mixture of **1** and **2** ([**1** + **2**] = 1.0×10^{-4} M) was placed in a 50 mL vial containing 7 mL of MeOH for vapor diffusion and allowed to stand at 25 °C. In two weeks, a yellow precipitate formed quantitatively, which consisted exclusively of nanotubes, as confirmed by scanning and transmission electron microscopy (Figures S1 and S2, Supporting Information).[5] Over a wide range of the molar ratio of **1** to **2** (mole fractions of **1** = 0.5, 1, 3, 10, 25, 50, 75, and 90%) and

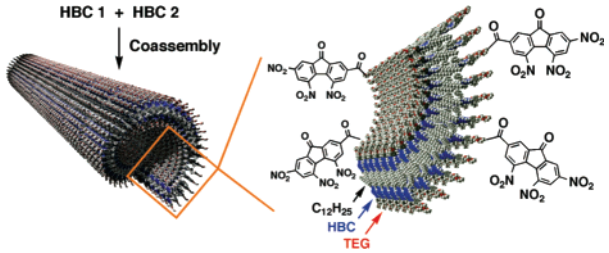

Figure 1. Schematic illustration for the formation of a coassembled graphitic nanotube from HBC **1** and **2**. TEG = triethylene glycol.

from **1** or **2** alone, nanotubes likewise formed under the vapor diffusion conditions described above (Figures S1 and S2).[5] In differential scanning calorimetry (DSC), all the nanotubes, irrespective of the content of **1**, exhibited a single endothermic peak (Figure S3a)[5] originating from the phase transition to a liquid crystalline mesophase.[4b] This is in sharp contrast with the phase transition profiles of the blended nanotubes of **1** and **2**, which showed multiple endothermic peaks over a broad temperature range from 175 to 218 °C (Figure S3b).[5] We also noticed that the transition temperatures of the nanotubes, formed from the mixtures of **1** and **2** (e.g., 196.2, 183.7, and 203.1 °C at the mole fractions of **1** = 25, 50, and 75%, respectively), are obviously lower than those of the parent homotropic nanotubes of **1** (214.0 °C) and **2** (207.1 °C). These DSC profiles indicate that **1** and **2** coassemble uniformly without forming their large homotropic domains. The successful nanotubular coassembly is worthwhile to note, since the diameters of the homotropic nanotubes of **1** (16 nm)[3] and **2** (20 nm)[4b] differ from one another. As the content of **1** increased from 0 to 100%, the diameter of the nanotubes decreased from 20 to 16 nm (Figure S4).[5] Such a design flexibility is remarkable and gives contrast to crystalline systems, where the composition of cocrystals are not easy to vary.

We found that the photoconductivity of the coassembled nanotubes displays a bell-shaped dependency on the mole fraction of **1**. Figure 2a shows transient profiles of the photoconductivity ($\phi\Sigma\mu$)[6] of the nanotubes with different mole fractions of **1**, evaluated by flash-photolysis time-resolved microwave conductivity (FP-TRMC) measurements.[5,7] The maximum photoconductivity ($\phi\Sigma\mu_{max}$) monotonically increased as the mole fraction of **1** increased from 0 to 75% and then decreased progressively (Figure 2b).[8] Noteworthy is that incorporation of only a small amount of **1** (e.g., 10%) into the nanotubes gave rise to an even greater $\phi\Sigma\mu_{max}$ value than that of the nanotubes composed of **1** alone.

[†] ERATO−SORST Nanospace Project (JST).
[‡] The University of Tokyo.
[§] Osaka University.
[#] Biological Information Research Center (AIST).

10.1021/ja073577q CCC: $37.00

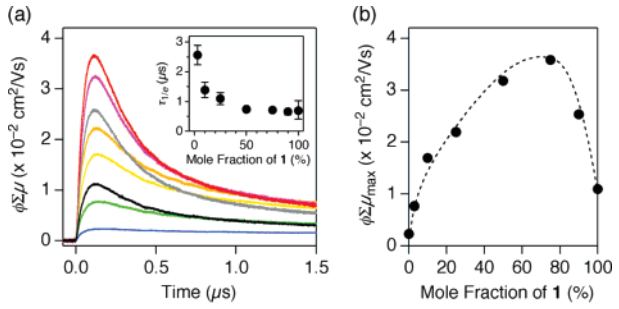

Figure 2. (a) FP-TRMC profiles of cast films of the nanotubes with varying mole fractions of **1**: 0 (blue), 3 (green), 10 (yellow), 25 (orange), 50 (purple), 75 (red), 90 (gray), and 100% (black), upon photoirradiation at 355 nm (photon density, 1.2×10^{15} cm^{-2}). Inset shows a plot of $\tau_{1/e}$ values versus mole fractions of **1**. (b) Plot of $\phi\Sigma\mu_{max}$ values versus mole fractions of **1**.

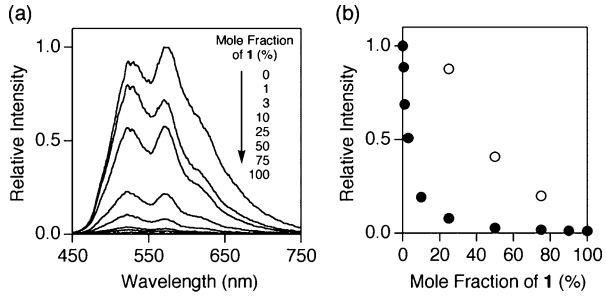

Figure 3. (a) Fluorescence spectra of cast films of the nanotubes with varying mole fractions of **1**; (b) plot of integral fluorescence intensities of the nanotubes (filled circles) and that of blended nanotubes of **1** and **2** (open circles) versus mole fractions of **1**. All the spectra were normalized relative to the 570 nm fluorescence intensity of the nanotubes of **2**.

While the π-stacked HBC units in the nanotubes of **2** can fluoresce, those in the nanotubes of **1** is not luminescent owing to a photoinduced electron transfer (PET) to the appended TNF units.[3] Since the fluorescence of the nanotubes of **2** was hardly quenched upon blending with the nanotubes of **1**, the intertubular PET can be negligible (Figure 3b, open circles). We also found that the fluorescence of **2** is progressively quenched upon coassembling with **1** (Figure 3a,b, filled circles). Of interest, only at a 10% mole fraction of **1**, nearly 80% of the fluorescence of **2** was quenched, indicating that anticipated reduction of the photocarrier generation yield (ϕ), on lowering the surface concentration of TNF, is much less. This is a great advantage of our system and most likely due to the occurrence of a rapid excitation energy migration in the graphitic layer of π-stacked HBC.[1e] In the meanwhile, a high acceptor concentration often promotes charge recombination, resulting in shortening the lifetime of the charge-separated state. However, as shown in Figure 2a (inset), the lifetime ($\tau_{1/e}$)[9] of the photogenerated charge carrier hardly changed over a wide range of the content of **1** (10−90%) and was comparable to that in the nanotubes of **1** (0.7 μs). This trend indicates that the designed segregation of the donor and acceptor layers in the nanotubes is enough to suppress the charge recombination.

We initially anticipated if the bell-shaped correlation between the photoconductivity ($\phi\Sigma\mu_{max}$) and content of **1** (Figure 2b) might be due to opposite dependencies of the photogeneration of charge carriers and their recombination on the concentration of TNF. Along this line, the increase in $\phi\Sigma\mu_{max}$ upon increment of the TNF concentration is reasonable, considering the enhanced HBC-to-TNF electron transfer. However, since the carrier lifetime is almost intact to the content of **1** (vide ante), the sudden drop of $\phi\Sigma\mu_{max}$, observed at the content of **1** from 75 to 100%, cannot be accounted for in terms of charge recombination. We assume if the charge carrier mobility ($\Sigma\mu$) of the graphitic layer may change with the density of the surrounding TNF units. As TNF is bulky, there must be an upper limit in the number of the TNF units that the nanotubes can accommodate on their surface without disruption.[3] Above this upper limit, the π-stacked HBC units start to undergo disordering, thereby leading to the reduction of $\Sigma\mu$. The bell-shaped dependency in Figure 2b indicates that this essential drawback can be avoided by the coassembly of **1** with a certain amount of HBC without TNF (**2**).

In conclusion, we succeeded in the coassembly of two different hexa-*peri*-hexabenzocoronenes, one possessing an electron-accepting TNF unit (**1**) and the other unfunctionalized (**2**), affording graphitic nanotubes with varying acceptor concentrations. Photoconducting properties of the nanotubes are greatly enhanced by incorporating an appropriate amount of **2** in the nanotubes of **1**. Advantageously, a rapid excitation energy migration in the graphitic layer of π-stacked HBC possibly occurs and contributes to the preservation of the high electron-transfer efficiency, to furnish the charge separation. Furthermore, a high concentration of TNF on the nanotube surface hardly promotes the charge recombination, thanks to the properly designed nanometer gap between the donor and acceptor layers. This achievement provides an important insight for the design of molecularly engineered optoelectronic materials with segregated donor−acceptor geometries.[10]

Supporting Information Available: Experimental details and supporting Figures S1−S4, including electron micrographs and DSC thermographs. This material is available free of charge via the Internet at http://pubs.acs.org.

References

(1) (a) Tang, C. W. *Appl. Phys. Lett.* **1986**, *48*, 183−185. (b) Yu, G.; Gao, J.; Hummelen, J. C.; Wudl, F.; Heeger, A. J. *Science*, **1995**, *270*, 1789−1791. (c) Granström, M.; Petritsch, K.; Arias, A. C.; Lux, A.; Andersson, M. R.; Friend, R. H. *Nature* **1998**, *395*, 257−260. (d) Schmidt-Mende, L.; Fechtenkötter, A.; Müllen, K.; Moons, E.; Friend, R. H.; MacKenzie, J. D. *Science* **2001**, *293*, 1119−1122. (e) Brédas, J.-L.; Beljonne, D.; Coropceanu, V.; Cornil, J. *Chem. Rev.* **2004**, *104*, 4971−5003. (f) Li, G.; Shrotriya, V.; Huang, J.; Yao, Y.; Moriarty, T.; Emery, K.; Yang, Y. *Nat. Mater.* **2005**, *4*, 864−868. (g) Scharber, M. C.; Mühlbacher, D.; Koppe, M.; Denk, P.; Waldauf, C.; Heeger, A. J.; Brabec, C. J. *Adv. Mater.* **2006**, *18*, 789−794. (h) Kim, Y.; Cook, S.; Tuladhar, S. M.; Choulis, S. A.; Nelson, J.; Durrant, J. R.; Bradley, D. D. C.; Giles, M.; Mcculloch, I.; Ha, C.-S.; Ree, M. *Nat. Mater.* **2006**, *5*, 197−203.

(2) (a) Samorì, P.; Yin, X.; Tchebotareva, N.; Wang, Z.; Pakula, T.; Jäckel, F.; Watson, M. D.; Venturini, A.; Müllen, K.; Rabe, J. P. *J. Am. Chem. Soc.* **2004**, *126*, 3567−3575. (b) Würthner, F.; Chen, Z.; Hoeben, F. J. M.; Osswald, P.; You, C.-C.; Jonkheijm, P.; Herrikhuyzen, J. V.; Schenning, A. P. H. J.; van der Schoot, P. P. A. M.; Meijer, E. W.; Beckers, E. H. A.; Meskers, S. C. J.; Janssen, R. A. J. *J. Am. Chem. Soc.* **2004**, *126*, 10611−10618. (c) Beckers, E. H. A.; Meskers, S. C. J.; Schenning, A. P. H. J.; Chen, Z.; Würthner, F.; Marsal, P.; Beljonne, D.; Cornil, J.; Janssen, R. A. J. *J. Am. Chem. Soc.* **2006**, *128*, 649−657.

(3) Yamamoto, Y.; Fukushima, T.; Suna, Y.; Ishii, N.; Saeki, A.; Seki, S.; Tagawa, S.; Taniguchi, M.; Kawai, T.; Aida, T. *Science* **2006**, *314*, 1761−1764.

(4) (a) Jin, W.; Fukushima, T.; Niki, M.; Kosaka, A.; Ishii, N.; Aida, T. *Proc. Natl. Acad. Sci. U.S.A.* **2005**, *102*, 10801−10806. (b) Hill, J. P.; Jin, W.; Kosaka, A.; Fukushima, T.; Ichihara, H.; Shimomura, T.; Ito, K.; Hashizume, T.; Ishii, N.; Aida, T. *Science* **2004**, *304*, 1481−1483.

(5) See Supporting Information.

(6) The photoconductivity ($\phi\Sigma\mu$) was obtained from the observed transient conductivity, where ϕ and $\Sigma\mu$ are photocarrier generation yield and sum of charge carrier mobility, respectively.[7]

(7) Acharya, A.; Seki, S.; Koizumi, Y.; Saeki, A.; Tagawa, S. *J. Phys. Chem. B* **2005**, *109*, 20174−20179.

(8) This trend was intact to the incident photon density ranging from 0.59×10^{15} to 5.9×10^{15} cm^{-2}.

(9) The lifetime ($\tau_{1/e}$) is defined as the time when $\phi\Sigma\mu$ decreases to 1/*e* of $\phi\Sigma\mu_{max}$.

(10) Schenning, A. P. H. J.; Meijer, E. W. *Chem. Commun.* **2005**, 3245−3258.

JA073577Q